

Effect of the adsorbate stiffness on the resonance response of microcantilever sensors

Javier Tamayo,^{a)} Daniel Ramos, Johan Mertens, and Montserrat Calleja
 Bionanomechanics Laboratory, IMM-CNM, CSIC, Isaac Newton 8, 28760 Tres Cantos, Spain

(Received 31 July 2006; accepted 4 October 2006; published online 1 December 2006)

The authors present a theoretical model to predict the resonance frequency shift due to molecule adsorption on micro- and nanocantilevers. They calculate the frequency shift experienced by cantilevers made of either silicon or the polymer SU-8, when two adsorbates, myosin protein and an alkanethiol, are attached to the cantilever surface. They demonstrate that the effect of the adsorbate stiffness can be comparable or even larger than the mass effect, producing positive frequency shifts. The results provide methods for decoupling both opposite effects and routes for the design of resonators with high sensitivity to molecule adsorption based on either stiffness or mass effects.
 © 2006 American Institute of Physics. [DOI: 10.1063/1.2388925]

Microcantilever resonators have been proposed for highly sensitive label-free detection of organic and biological molecules.^{1–3} The basic principle is the measurement of the resonance frequency shift due to the added mass of the molecules bound to the cantilever surface. The sensitivity is inversely proportional to the active mass of the resonator. Advances in micro- and nanofabrication techniques have motivated an intense effort for scaling the resonator size down in order to push the detection limits.^{2,3} Thus the sensitivity of the technique has rapidly evolved from the picogram to the attogram range, by simply reducing the size of the resonators (length \times width \times thickness) from $(100–500) \times (20–100) \times (0.5–1)$ to $(5–20) \times (0.5–2) \times (0.1–0.3) \mu\text{m}^3$. Consequently, the resonance frequency increases from the kilohertz to the megahertz regime. By further reduction of the size to the nanoscale, the detection limits can achieve unprecedented values.³

Independently of the cantilever size, the quantification of the adsorbed mass is an issue still not resolved. First, when the molecules are not uniformly adsorbed, the resonance frequency critically depends on the distribution of the molecules on the resonator.^{4,5} Second, a discrepancy is, in many cases, found between the added mass calculated by the theory and the mass adsorbed on the cantilever. This discrepancy is generally justified by invoking the effect of the adsorption-induced surface stress on the resonance frequency.⁶ In this effect, the surface stress is simplified to an external axial force that creates a shearing moment. Recently, Lu *et al.*⁷ have demonstrated that this model is inadequate to describe the physical system because in the real situation, the cantilever free end allows the deformation to relieve the stress. In their theoretical treatment, a strain-dependent surface stress is necessary to observe some effect on the resonant frequency, and therefore the surface stress effect is expected to be negligible in biomolecular applications.

Up to date, the influence of the mechanical properties of the adsorbed molecules on the resonance has been neglected. In this work, we present a theoretical model to study the effect of the stiffness of the molecules bound to a microcantilever on the resonance frequency. We demonstrate that this effect is comparable to the added mass effect.

A schematic depiction of the resonator modeled in the theoretical calculations is shown in Fig. 1. The resonator is a singly clamped cantilever of length L , width W , and thickness T_c , oriented along the x axis with flexural displacement along the z axis. The origin of the x axis is situated at the clamping. The schematic depicts the targeted molecules trapped on the cantilever as a layer of thickness T_a that depends on the x coordinate. The Young's modulus and density of the cantilever material and adsorbates are E_c , ρ_c , E_a , and ρ_a , respectively. We assume that adsorbates are homogeneously distributed across the width of the beam.

Neglecting rotatory inertia and shear deformation, the flexural displacement $u(x,t)$ obeys the differential equation,

$$W(\rho_c T_c + \rho_a T_a(x)) \frac{\partial^2 u(x,t)}{\partial t^2} + \frac{\partial^2}{\partial x^2} \left(D(x) \frac{\partial^2 u(x,t)}{\partial x^2} \right) = 0, \quad (1)$$

where $D(x)$ is the flexural rigidity of the cantilever given by⁸

$$D(x) = \frac{D_0}{1 + (E_a/E_c)(T_a(x)/T_c)} \{ 1 + (E_a/E_c)^2 (T_a(x)/T_c)^4 + 2(E_a/E_c)(T_a(x)/T_c)[2 + 3T_a(x)/T_c + 2(T_a(x)/T_c)^2] \}, \quad (2)$$

where $D_0 = (1/12)E_c W T_c^3$ is the flexural rigidity of the unloaded cantilever. Since Eq. (1) cannot be analytically solved in a general situation, we have calculated the resonance frequencies of the system by performing an energy-work balance during a vibration cycle.⁹ The accuracy of the method depends on how closely one can predict the vibration shape. In this model, we assume that molecules adsorbed on the cantilever negligibly change the eigenmode shape. We can then assume a harmonic transverse vibration given by $u(x,t) = A \psi_n(x) \cos(\omega_n t + \phi)$, where ψ_n is the n th eigenmode shape of the unloaded cantilever, ω_n is the n th eigenfrequency of the loaded cantilever, and A and ϕ are arbitrary values of the amplitude and phase. The mean values of the beam bending work and kinetic energy per oscillation cycle are, respectively, given by

$$\langle W_s \rangle = \frac{A^2}{4} \int_0^L D(x) \dot{\psi}_n^2(x) dx, \quad (3a)$$

^{a)}Electronic mail: jtamayo@imm.cnm.csic.es

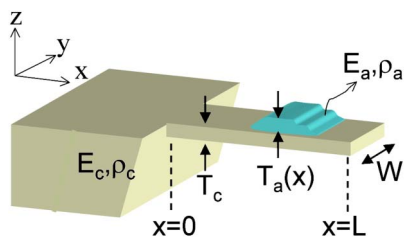


FIG. 1. Schematic depiction of a singly clamped cantilever with molecules adsorbed on its surface.

$$\langle W_k \rangle = \frac{WA^2}{4} \omega_n^2 \int_0^L (\rho_c T_c + \rho_a T_a(x)) \psi_n^2(x) dx. \quad (3b)$$

The eigenmode shapes of the unloaded cantilever are given by⁹

$$\begin{aligned} \psi_n(x) = & \sin(\beta_n x/L) - \sinh(\beta_n x/L) \\ & + \frac{\sin \beta_n + \sinh \beta_n}{\cos \beta_n + \cosh \beta_n} [\cosh(\beta_n x/L) - \cos(\beta_n x/L)], \end{aligned} \quad (4)$$

where the eigenvalues β_n satisfy the equation $1 + \cos \beta_n \cosh \beta_n = 0$. The first eigenvalues are given by $\beta_n = 1.8751, 4.6941, 7.8548, \dots$. We express the curvature as function of the unitless function $\phi_n(x) = L^2 \ddot{\psi}_n(x)$. By equaling Eqs. (3a) and (3b), the resonant frequency is calculated as

$$\omega_n^2 = \frac{(1/L^3) \int_0^L D(x) \phi_n^2(x) dx}{m_c \int_0^L (1 + (\rho_a/\rho_c)[T_a(x)/T_c]) \psi_n^2(x) dx}, \quad (5)$$

where m_c is the mass of the beam.

We will analyze first the effect of a homogeneous adsorbate layer on the cantilever. Equation (5) can be written in powers of T_a/T_c ,

$$\frac{\omega_n - \omega_{0n}}{\omega_{0n}} \cong \alpha_1 \left(\frac{T_a}{T_c} \right) + \alpha_2 \left(\frac{T_a}{T_c} \right)^2, \quad (6a)$$

$$\alpha_1 = \frac{1}{2} \left(3 \frac{E_a}{E_c} - \frac{\rho_a}{\rho_c} \right), \quad (6b)$$

$$\alpha_2 = \frac{3}{8} \left[\left(\frac{\rho_a}{\rho_c} \right)^2 + 2 \frac{E_a}{E_c} \left(4 - \frac{\rho_a}{\rho_c} \right) - 7 \left(\frac{E_a}{E_c} \right)^2 \right], \quad (6c)$$

where ω_{0n} is the unloaded eigenfrequency. In many cases, the layer formed by the adsorbed molecules is much thinner than the cantilever. The relative frequency shift can be then characterized by the proportionality constant α_1 . Thus, the resonance frequency shift is the result of the addition of two linear effects, the stiffness of the layer [first summand in Eq. (6b)] that produces a positive shift of the resonance frequency, and the well-known effect of the added mass [second summand in Eq. (6b)] that shifts the resonance to a lower frequency. However, as the size of the resonators is being increasingly reduced, the thickness of the adsorbed layer is getting comparable to the cantilever thickness, bringing about nonlinear effects and the coupling of the stiffness and mass effects as shown below.

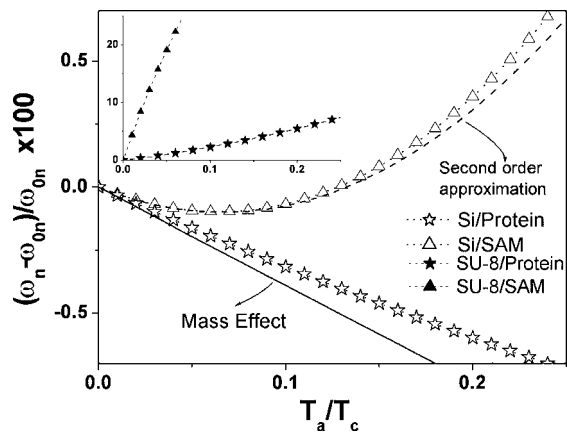


FIG. 2. Relative eigenfrequency shift vs ratio between the thickness of the uniformly adsorbed layer and the cantilever.

Figure 2 shows the relative frequency shift calculated from Eq. (5) for two cantilever materials and two organic and biological adsorbed layers. As cantilever materials we have chosen silicon ($\rho_c = 2330 \text{ kg/m}^3$, $E_c = 169 \text{ GPa}$) and the photoresist SU-8 ($\rho_c = 1190 \text{ kg/m}^3$, $E_c = 4.0 \text{ GPa}$).¹⁰ As paradigmatic organic and biological layers on the cantilever, we have chosen the self-assembled monolayer (SAM) formed by the alkanethiol $-\text{SH}-(\text{CH}_2)_{11}-\text{CH}_3$ ($\rho_a = 675 \text{ kg/m}^3$, $E_a = 12.9 \text{ GPa}$) and the monolayer formed by the myosin subfragment 1 ($\rho_a = 183 \text{ kg/m}^3$, $E_a = 0.7 \text{ GPa}$). The mechanical properties of these films were obtained from monolayers with a thickness of few nanometers via force-based techniques.^{11,12} The adsorption of the protein layer on the silicon cantilever produces a decrease of the resonance frequency that is approximately linear with the amount of adsorption (Fig. 2, open stars). Interestingly, the added mass would be underestimated about 18% if the effect of the layer stiffness would be neglected (Fig. 2, continuous line). For the highly packed SAM on the silicon cantilever, the contribution of the stiffness becomes more important and the resulting curve shows a more complex behavior (Fig. 2, open triangles). For $T_a/T_c < 0.04$ the resonance frequency decreases approximately linearly, indicating that the mass effect dominates for small thicknesses. In an intermediate regime between $T_a/T_c = 0.04$ and 0.1 , the contributions of the monolayer stiffness and added mass practically cancel each other and the resonance frequency is practically insensitive to adsorption. For values of $T_a/T_c > 0.1$ the resonance frequency and its slope increase with T_a/T_c , implying that the stiffness effect dominates over the added mass. The complex pattern exhibited in this curve can be accurately fitted with the simple second order approximation expressed in Eq. (6) (dashed line). When the cantilevers are fabricated in SU-8, the stiffness of the adsorbed film dominates the resonance response due to the low Young's modulus of SU-8 (Fig. 2, inset). Thus the adsorption of both films produces large positive frequency shifts.

Let us now study the case in which the adsorbed molecules are located on a region whose position coordinate and width are given by x_0 and Δx_i respectively. Figure 3 shows the adsorption position dependence of the first mode relative resonance frequency shift for the proteins described above on silicon and SU-8 cantilevers. Here, $\Delta x/L = 0.1$ and $T_a/T_c = 0.1$ and the frequency is numerically calculated by using Eq. (5). For both cantilever materials, the resonance fre-

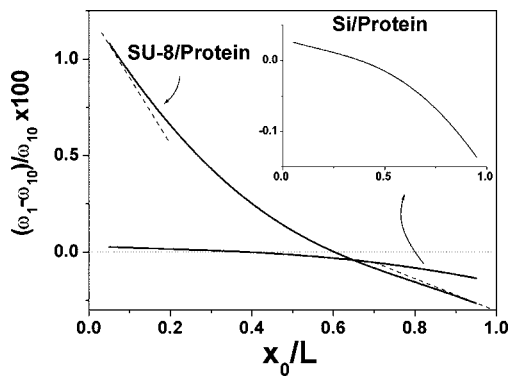


FIG. 3. Relative resonance frequency shift for the fundamental mode due to the adsorption of the myosin subfragment 1 as a function of the adsorption position along the cantilever normalized to the cantilever length. Two cantilever materials are modeled, SU-8 and silicon. The inset shows a zoom of the curve corresponding to the silicon cantilever.

quency shift is positive when the proteins are positioned near the clamping and it monotonically decreases up to be negative at the free cantilever end. This behavior is understood through the proportionality constants for the change of the mass and flexural rigidity in Eq. (5), $\psi_n^2(x_0)$ and $\phi_n^2(x_0)$, respectively. These quantities, respectively, correspond with the square values of the amplitude and curvature of the vibration shape at the adsorption position. When the proteins are positioned near the clamping $\psi_1^2 \cong 0$ whereas ϕ_1^2 reaches its maximal value, and conversely, when the proteins are near the free end $\phi_1^2 \cong 0$ and ψ_1^2 is maximal. For both cases, we provide useful simple approximate expressions to relate the resonance frequency with the increase of stiffness and mass,

$$\frac{\omega_1}{\omega_{01}} \cong \left(1 + f \left(\frac{L-x_0}{x_0} \right) \frac{m_a}{m_c} \right)^{-1/2} \quad \text{for } x_0 \cong L, \quad (7a)$$

$$\frac{\omega_1}{\omega_{01}} \cong \left(1 + f \left(\frac{x_0}{L} \right) \frac{D-D_0}{D} \frac{\Delta x}{L} \right)^{1/2} \quad \text{for } x_0 \cong 0, \quad (7b)$$

where the function $f(z) = 4.000 - 11.012z$ accounts for small deviations of the adsorption position with respect to the fixed or free ends of the cantilever. Both approximated expressions are plotted in Fig. 3 at both ends (dashed lines) and they show a good agreement with the theoretical values of the resonance frequency obtained from Eq. (5).

Due to the low Young's modulus of the SU-8, the adsorption of the proteins produces positive frequency shifts from $x_0=0$ to $x_0=0.60L$, whereas the crossover position for silicon is $x_0=0.38L$. By positioning the proteins near the clamping, the protein adsorption produces a positive relative frequency shift due to the stiffness of the adsorbates of about 1.1% whereas for the silicon cantilever this is about 40 times lower. Similarly, when the proteins are located at the cantilever free end, the added mass produces a negative relative frequency shift of 0.27% in the SU-8 cantilever and of 0.14% in the silicon cantilever. To compare the performance

of Si and SU-8 resonators with identical dimensions, an analysis of the frequency noise must be performed. If the noise is dominated by the displacement sensor and readout circuitry, the frequency noise can be assumed constant and independent of the resonator material. Then the sensitivity is given by the absolute values of the frequency shift, which can be compared by multiplying the relative resonance frequency shift by the factor $(E_c/\rho_c)^{0.5}$ that is about 4.6 times higher for silicon than for SU-8. If the noise is dominated by the intrinsic thermomechanical fluctuations, the frequency noise can approximately be written as $\delta\omega_0^2 \approx k_B T \Delta f / (m^* \omega_0 \langle z^2 \rangle Q)$.³ Here, k_B is Boltmann's constant, T is the resonator temperature, $\langle z^2 \rangle$ is the mean square amplitude, Δf is the measurement bandwidth, and $m^* \cong 0.243m_c$ is the effective mass of the resonator. The ratio between the absolute resonance frequency shift and the frequency noise is the figure of merit to compare performances. By introducing the material properties, the ratio between the frequency noises of SU-8 and Si resonators with identical dimensions is $(\delta\omega_{0,SU-8}/\delta\omega_{0,Si}) \approx 3(Q_{Si}/Q_{SU-8})^{0.5}$. For resonators in gas or liquid, the energy loss is dominated by the viscous damping and $Q \approx T_c \rho_c / 3 \{ \omega_0 / (2\rho_{fluid}) \}^{0.5}$, where η and ρ_{fluid} are the viscosity and density of the fluid. In this case $Q_{Si}/Q_{SU-8} \approx 4.2$, resulting $(\delta\omega_{0,SU-8}/\delta\omega_{0,Si}) \approx 6.2$.¹³

The presented work clearly shows the important influence of Young's modulus of the adsorbates in the response of biological and chemical sensors based on micro- and nano-mechanical resonators. The calculations show how the opposite contributions of the added mass and stiffness can cancel each other producing small responses. Both effects can be decoupled by confining the adsorption to defined areas of the resonator. The result point at polymer materials, such as SU-8, as good candidates for future resonating sensors with enhanced sensitivity based on molecule stiffness.

¹N. V. Lavrik, M. J. Stepaniak, and P. G. Datskos, Rev. Sci. Instrum. **75**, 2229 (2004).

²B. Illic, Y. Yang, K. Aubin, R. Reichenbach, S. Krylov, and H. G. Craighead, Nano Lett. **5**, 925 (2005).

³K. L. Ekinci and M. L. Roukes, Rev. Sci. Instrum. **76**, 061101 (2005).

⁴S. Dohn, R. Sandberg, W. Svendsen, and A. Boisen, Appl. Phys. Lett. **86**, 233501 (2005).

⁵D. Ramos, J. Tamayo, J. Mertens, M. Calleja, and A. Zaballos, J. Appl. Phys. (to be published).

⁶G. Y. Chen, T. Thundat, E. A. Wachter, and R. J. Warmack, J. Appl. Phys. **77**, 3618 (1995).

⁷P. Lu, H. P. Lee, C. Lu, and S. J. O'Shea, Phys. Rev. B **72**, 085405 (2005).

⁸R. Sandberg, W. Svendsen, K. Molhave, and A. Boisen, J. Micromech. Microeng. **15**, 1454 (2005).

⁹N. G. Stephen, J. Sound Vib. **131**, 345 (1989).

¹⁰M. Calleja, J. Tamayo, M. Nordstrom, and A. Boisen, Appl. Phys. Lett. **88**, 113901 (2006).

¹¹A. R. Burns, J. E. Houston, R. W. Carpick, and T. A. Michalasko, Langmuir **15**, 2922 (1999).

¹²H. Suda, Y. C. Sasaki, N. Oishi, N. Hiraoka, and K. Sutoh, Biochem. Biophys. Res. Commun. **261**, 276 (1999).

¹³J. F. Vignola, J. A. Judge, J. Jarzynski, M. Zalalutdinov, B. H. Houston, and J. W. Baldwin, Appl. Phys. Lett. **88**, 041921 (2006).